J|A|C|S ARTICLES

Published on Web 06/18/2009

Temperature Dependence of Blue Phosphorescent Cyclometalated Ir(III) Complexes

Tissa Sajoto,[†] Peter I. Djurovich,*[,†] Arnold B. Tamayo,[†] Jonas Oxgaard,[‡] William A. Goddard III,[‡] and Mark E. Thompson*[,†]

Department of Chemistry, University of Southern California, Los Angeles, California 90089, and Department of Chemistry, California Institute of Technology, Pasadena, California 91125

Received April 24, 2009; E-mail: djurovic@usc.edu; met@usc.edu

Abstract: The photophysical properties for a series of facial (*fac*) cyclometalated Ir(III) complexes (*fac*-Ir(C^N)$_3$ (C^N = 2-phenylpyridyl (ppy), 2-(4,6-difluorophenyl)pyridyl (F2ppy), 1-phenylpyrazolyl (ppz), 1-(2,4-difluorophenyl)pyrazolyl) (F2ppz), and 1-(2-(9,9′-dimethylfluorenyl))pyrazolyl (flz)), *fac*-Ir(C^N)$_2$(C^N′) (C^N = ppz or F2ppz and C^N′ = ppy or F2ppy), and *fac*-Ir(C^C′)$_3$ (C^C′ = 1-phenyl-3-methylbenzimidazolyl (pmb)) have been studied in dilute 2-methyltetrahydrofuran (2-MeTHF) solution in a temperature range of 77−378 K. Photoluminescent quantum yields (Φ) for the 10 compounds at room temperature vary between near zero and unity, whereas all emit with high efficiency at low temperature (77 K). The quantum yield for *fac*-Ir(ppy)$_3$ (Φ = 0.97) is temperature-independent. For the other complexes, the temperature-dependent data indicates that the luminescent efficiency is primarily determined by thermal deactivation to a nonradiative state. Activation energies and rate constants for both radiative and nonradiative processes were obtained using a Boltzmann analysis of the temperature-dependent luminescent decay data. Activation energies to the nonradiative state are found to range between 1600 and 4800 cm^{-1}. The pre-exponential factors for deactivation are large for complexes with C^N ligands ($10^{11}-10^{13}$ s^{-1}) and significantly smaller for *fac*-Ir(pmb)$_3$ (10^9 s^{-1}). The kinetic parameters for decay and results from density functional theory (DFT) calculations of the triplet state are consistent with a nonradiative process involving Ir−N (Ir−C for *fac*-Ir(pmb)$_3$) bond rupture leading to a five-coordinate species that has triplet metal-centered (^{3}MC) character. Linear correlations are observed between the activation energy and the energy difference calculated for the emissive and ^{3}MC states. The energy level for the ^{3}MC state is estimated to lie between 21 700 and 24 000 cm^{-1} for the *fac*-Ir(C^N)$_3$ complexes and at 28 000 cm^{-1} for *fac*-Ir(pmb)$_3$.

Introduction

Cyclometalated iridium(III) complexes have been recently shown to have phosphorescence efficiencies approaching theoretical limits (Φ = 0.8−1.0) and short radiative triplet lifetimes (τ = 1−5 μs).[1,2] These photophysical properties make organometallic Ir complexes excellent candidates for use in oxygen detection,[3] metal ion sensing,[4,5] and luminescent labeling reagents for biological materials;[6−20] however, the most extensively investigated application of cyclometalated Ir(III) complexes is as emitters in organic light-emitting diodes (OLEDs).[21] The high phosphorescent efficiencies, short lifetimes, and broad range of emission colors make these Ir(III) complexes ideal emitters in OLEDs, designed for flat panel displays and white

[†] University of Southern California.
[‡] California Institute of Technology.

(1) Endo, A.; Suzuki, K.; Yoshihara, T.; Tobita, S.; Yahiro, M.; Adachi, C. *Chem. Phys. Lett.* **2008**, *460*, 155–157.
(2) You, Y.; Park, S. Y. *Dalton Trans.* **2009**, 1267–1282.
(3) Borisov, S. M.; Klimant, I. *Anal. Chem.* **2007**, *79*, 7501–7509.
(4) Zhao, Q.; Liu, S. J.; Li, F. Y.; Yi, T.; Huang, C. H. *Dalton Trans.* **2008**, 3836–3840.
(5) Schmittel, M.; Lin, H. W. *Inorg. Chem.* **2007**, *46*, 9139–9145.
(6) Yu, M. X.; Zhao, Q.; Shi, L. X.; Li, F. Y.; Zhou, Z. G.; Yang, H.; Yia, T.; Huang, C. H. *Chem. Commun.* **2008**, 2115–2117.
(7) Lo, K. K. W.; Zhang, K. Y.; Leung, S. K.; Tang, M. C. *Angew. Chem., Int. Ed.* **2008**, *47*, 2213–2216.
(8) Lo, K. K. W.; Lee, P. K.; Lau, J. S. Y. *Organometallics* **2008**, *27*, 2998–3006.
(9) Elias, B.; Genereux, J. C.; Barton, J. K. *Angew. Chem., Int. Ed.* **2008**, *47*, 9067–9070.
(10) Shao, F. W.; Elias, B.; Lu, W.; Barton, J. K. *Inorg. Chem.* **2007**, *46*, 10187–10199.
(11) Shao, F. W.; Barton, J. K. *J. Am. Chem. Soc.* **2007**, *129*, 14733–14738.
(12) Lo, K. K. W.; Zhang, K. Y.; Chung, C. K.; Kwok, K. Y. *Chem.—Eur. J.* **2007**, *13*, 7110–7120.
(13) Lo, K. K. W.; Tsang, K. H. K.; Sze, K. S.; Chung, C. K.; Lee, T. K. M.; Zhang, K. Y.; Hui, W. K.; Li, C. K.; Lau, J. S. Y.; Ng, D. C. M.; Zhu, N. *Coord. Chem. Rev.* **2007**, *251*, 2292–2310.
(14) Lo, K. K. W.; Lau, J. S. Y. *Inorg. Chem.* **2007**, *46*, 700–709.
(15) Lo, K. K. W. In *Photofunctional Transition Metals Complexes*; Yam, V. W. W., Ed.; Structure and Bonding, Vol. 123; Springer: Berlin, Heidelburg, New York, 2007; pp 205−245.
(16) Lo, K. K. W.; Lau, J. S. Y.; Lo, D. K. K.; Lo, L. T. L. *Eur. J. Inorg. Chem.* **2006**, *405*, 4–4062.
(17) Lo, K. K. W.; Hui, W. K.; Chung, C. K.; Tsang, K. H. K.; Lee, T. K. M.; Li, C. K.; Lau, J. S. Y.; Ng, D. C. M. *Coord. Chem. Rev.* **2006**, *250*, 1724–1736.
(18) Lo, K. K. W.; Chung, C. K.; Zhu, N. Y. *Chem.—Eur. J.* **2006**, *12*, 1500–1512.
(19) Lo, K. K. W.; Li, C. K.; Lau, J. S. Y. *Organometallics* **2005**, *24*, 4594–4601.
(20) Lo, K. K. W.; Hui, W. K.; Chung, C. K.; Tsang, K. H. K.; Ng, D. C. M.; Zhu, N. Y.; Cheung, K. K. *Coord. Chem. Rev.* **2005**, *249*, 1434–1450.
(21) Thompson, M. E.; Djurovich, P. I.; Barlow, S.; Marder, S. R. In *Comprehensive Organometallic Chemistry*; O'Hare, D., Ed.; Elsevier: Oxford, 2007; Vol. 12, pp 101−194.

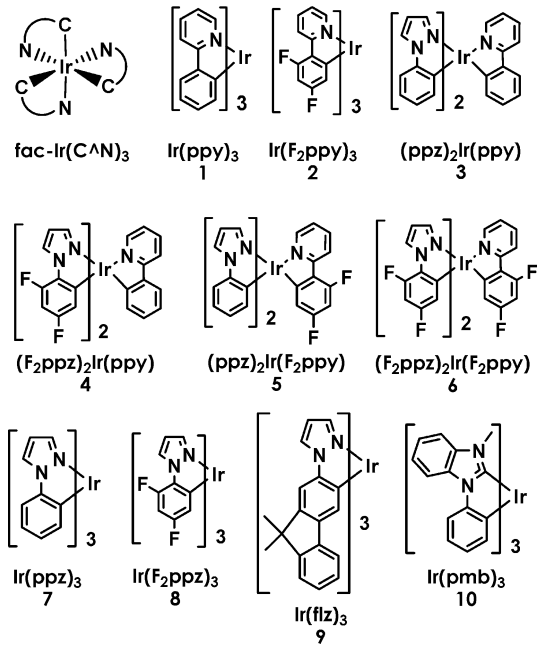

Figure 1. Molecular structures of the Ir complexes used in this study. All complexes are facial (*fac*) isomers.

light sources.[22,23] Although a wide range of Ir(III) materials have been reported that emit from blue to the near-infrared, the number of highly efficient, blue-to-violet phosphorescent Ir(III) complexes are limited and their photophysical properties are not fully understood. In present study we have focused our attention on Ir(III) complexes with emission energies ranging from the near-UV to green in order to develop a better understanding of the processes that limit the luminescent efficiency from this class of materials.

Blue phosphorescence can be observed from Ir(III) complexes that have cyclometalated phenylpyridine (ppy) ligands modified to increase the emission energy relative to that of an efficient green phosphor, *fac*-Ir(ppy)$_3$ (**1**, Figure 1). For example, addition of electron-withdrawing groups such as fluorine leads to a complex, *fac*-Ir(F$_2$ppy)$_3$ (**2**), that displays emission 40 nm higher in energy compared to **1**.[24] Similarly, a difluorinated bipyridine ligand has recently been used to form a tris-cyclometalated Ir(III) complex that displays blue phosphorescence.[25] Homoleptic complexes using non-pyridine-based heterocyclic ligands that have high triplet energies, such as phenylpyrazole,[11] phenyltriazole,[12] pyridylazolate,[26] phenylimidazole, or phenylbenzimidazole,[13] likewise phosphoresce at high energy. Other examples include heteroleptic derivatives that use electron-withdrawing ancillary ligand(s) to raise the emission energy by stabilizing the highest occupied molecular orbital (HOMO).[27−33] Although cyclometalated Ir(III) complexes with high emission energies can be obtained using any of these approaches, the luminescent efficiencies are often well below that of **1** due to a significant increase in nonradiative decay rates. A more detailed picture of the excited-state processes is thus needed in order to optimize the phosphorescent behavior of this class of materials.

Key information about the photophysical properties of phosphorescent transition metal complexes can be obtained by studying the temperature dependence of emission from these materials. In particular, analysis of temperature-dependent transient decay from diimine (i.e., bipyridine, bpy) chelates of Ru(II) and Os(II) with metal-to-ligand charge transfer (MLCT) excited states has enabled detailed characterization the radiative and nonradiative states.[34−38] Different types of behavior are observed for these compounds in two distinct temperature regimes. At low temperatures (0−77 K), the radiative rates are found to vary due to differing thermal population of three triplet substates. The effect comes about because a significant energy gap separates the lowest and highest substate. The energy difference between the two states in the absence of an external magnetic field is defined as the zero-field splitting (zfs).[39] The zfs values for the metal complexes are enhanced due to mixing of singlet and triplet states induced by spin−orbit coupling from the heavy metal ions. For example, the zfs values for Ru(bpy)$_3$ derivatives ($\sim$60 cm^{-1})[37] and Os(II) analogues (>200 cm^{-1})[38] are markedly larger than those found in organic molecules (typically 0.2 cm^{-1}).[39] At higher temperatures (77−300 K), variation in the nonradiative rates for Ru(II) and Os(II) complexes reveals the existence of thermally accessible, higher-lying excited states.[34,35,40,41] These higher-lying states typically reside ca. 2000 cm^{-1} above the MLCT state and provide a significant contribution to the loss of luminescent efficiency at room temperature. For polypyridyl complexes of Ru(II), nonradiative decay occurs through a triplet metal-centered (^{3}MC) ligand field state.[42] In contrast, the larger ligand field splitting of Os(II) complexes makes the ^{3}MC state relatively inaccessible at room temperature.[43] The Os(II) complexes instead suffer more severely from temperature-independent nonradiative decay.[44,45] The temperature depen-

(22) *Highly Efficient OLEDs with Phosphorescent Materials*; Yersin, H., Ed.; Wiley-VCH: Berlin, 2007.
(23) Yersin, H. *Top. Curr. Chem.* **2004**, *241*, 1–26.
(24) Tamayo, A. B.; Alleyne, B. D.; Djurovich, P. I.; Lamansky, S.; Tsyba, I.; Ho, N. N.; Bau, R.; Thompson, M. E. *J. Am. Chem. Soc.* **2003**, *125*, 7377–7387.
(25) Lee, S. J.; Park, K. M.; Yang, K.; Kang, Y. *Inorg. Chem.* **2009**, *48*, 1030–1037.
(26) Yeh, Y. S.; Cheng, Y. M.; Chou, P. T.; Lee, G. H.; Yang, C. H.; Chi, Y.; Shu, C. F.; Wang, C. H. *ChemPhysChem* **2006**, *7*, 2294–2297.
(27) Stagni, S.; Colella, S.; Palazzi, A.; Valenti, G.; Zacchini, S.; Paolucci, F.; Marcaccio, M.; Albuquerque, R. O.; De Cola, L. *Inorg. Chem.* **2008**, *47*, 10509–10521.
(28) Song, Y. H.; Chiu, Y. C.; Chi, Y.; Cheng, Y. M.; Lai, C. H.; Chou, P. T.; Wong, K. T.; Tsai, M. H.; Wu, C. C. *Chem.—Eur. J.* **2008**, *14*, 5423–5434.
(29) Orselli, E.; Albuquerque, R. Q.; Fransen, P. M.; Frohlich, R.; Janssen, H. M.; De Cola, L. *J. Mater. Chem.* **2008**, *18*, 4579–4590.
(30) Di Censo, D.; Fantacci, S.; De Angelis, F.; Klein, C.; Evans, N.; Kalyanasundaram, K.; Bolink, H. J.; Gratzel, M.; Nazeeruddin, M. K. *Inorg. Chem.* **2008**, *47*, 980–989.
(31) Chang, C. F.; Cheng, Y. M.; Chi, Y.; Chiu, Y. C.; Lin, C. C.; Lee, G. H.; Chou, P. T.; Chen, C. C.; Chang, C. H.; Wu, C. C. *Angew. Chem., Int. Ed.* **2008**, *47*, 4542–4545.
(32) Li, J.; Djurovich, P. I.; Alleyne, B. D.; Yousufuddin, M.; Ho, N. N.; Thomas, J. C.; Peters, J. C.; Bau, R.; Thompson, M. E. *Inorg. Chem.* **2005**, *44*, 1713–1727.
(33) Yang, C.-H.; Li, S.-W.; Chi, Y.; Cheng, Y.-M.; Yeh, Y.-S.; Chou, P.-T.; Lee, G.-H.; Wang, C.-H.; Shu, C.-F. *Inorg. Chem.* **2005**, *44*, 7770–7780.
(34) Allsopp, S. R.; Cox, A.; Kemp, T. J.; Reed, W. J. *J. Chem. Soc., Faraday Trans. 1* **1978**, *74*, 1275–1289.
(35) Van Houten, J.; Watts, R. J. *J. Am. Chem. Soc.* **1976**, *98*, 4853–4858.
(36) Hager, G. D.; Watts, R. J.; Crosby, G. A. *J. Am. Chem. Soc.* **1975**, *97*, 7037–7042.
(37) Hager, G. D.; Crosby, G. A. *J. Am. Chem. Soc.* **1975**, *97*, 7031–7037.
(38) Yersin, H.; Humbs, W.; Strasser, J. *Top. Curr. Chem.* **1997**, *191*, 153–249.
(39) Turro, N. J. *Modern Molecular Photochemistry*; Benjamin/Cummings: Menlo Park, CA, 1978.
(40) Barigelletti, F.; Juris, A.; Balzani, V.; Belser, P.; Vonzelewsky, A. *J. Phys. Chem.* **1986**, *90*, 5190–5193.
(41) Allsopp, S. R.; Cox, A.; Kemp, T. J.; Reed, W. J.; Carassiti, V.; Traverso, O. *J. Chem. Soc., Faraday Trans. 1* **1979**, *75*, 353–362.
(42) Meyer, T. J. *Pure Appl. Chem.* **1986**, *58*, 1193–1206.

dence of luminescent cyclometalated Pd(II), Rh(III), Pt(II), and Pt(IV) complexes has also been investigated, and these compounds show behavior similar to that of the Ru(II) and Os(II) complexes.[46]

Temperature-dependent luminescent studies have also been carried out on cyclometalated Ir(III) complexes. Complexes examined at cryogenic temperatures show temperature-dependent variations in radiative rates similar to that seen in Ru(II) and Os(II) bisiimine complexes.[47−51] Several tris(pyridylazolate) and tris(phenyltriazolate) Ir(III) complexes have been investigated at higher temperatures, and the presence of thermally activated, nonradiative processes in these species was shown to greatly diminish the luminescent efficiency at room temperature.[26,33,52,53] Of particular note is a recent report of a blue emissive Ir complex characterized by a temperature-dependent study along with theoretical calculation of the potential energy surface for the excited state.[54] The calculations were used to determine the metal−ligand distortions the complex undergoes as it proceeds along the deactivation pathway. Good agreement was found between the experimental and calculated energies for deactivation. In the present paper, we utilize temperature-dependent luminescent studies in conjunction with theoretical calculations to examine the radiative and nonradiative properties for cyclometalated Ir(III) complexes, **1**−**10** (Figure 1). We have measured the activation energies and kinetic parameters for deactivation of the excited state. Our analysis indicates that thermal population to a ^{3}MC state is the most likely deactivation processes for high-energy cyclometalated Ir(III) complexes. We use the results from both experimental and theoretical calculations to estimate the energies for the ^{3}MC state. The relative energy of the ^{3}MC state with respect to the emissive state is shown to be the principal factor that dictates the quantum efficiency for these blue cyclometalated Ir complexes.

Experimental Section

Synthesis. Compounds **1**−**10**, were prepared as previously described.[24,55]

Quantum Yield Measurement. The luminescent quantum yields of **1**−**10** were measured using an absolute method[56] more reliant than the relative method[57] typically employed in earlier studies. Measurements were carried out using a Hamamatsu C9920 system equipped with a xenon lamp, calibrated integrating sphere and model C10027 photonic multichannel analyzer. Dilute solutions ($\sim 10^{-5}$ M) of the compounds in 2-methyltetrahydrofuran (2-MeTHF) were placed in 1 cm^2 quartz cuvettes that were fitted with a Teflon stopcocks. Samples were deaerated by vigorously bubbling dry N_2 into the solutions using a flexible tube that was threaded through a center bore in the stopcock. It is worth noting that rubber septa were ineffective as seals for the optical cells and their use led to decreased quantum yields in less than 1 h after degassing. The quantum efficiencies were measured using either a 330 nm (for **10**) or 380 nm (for **1**−**6** and **9**) excitation wavelengths. The quantum efficiency data was processed using the U6039-05 software package provided by Hamamatsu. The reproducibility in the quantum efficiency measurements is ±5%.

Emission Intensity Measurement. Steady-state emission measurements were performed using a QuantaMaster model C-60SE spectrofluorimeter (Photon Technology International) with an excitation wavelength of 360 nm. The emission intensity measurement experiments of *fac*-Ir(ppy)$_3$ were carried out in dilute ($\sim 10^{-5}$ M), N_2-degassed 2-MeTHF solution using a custom Dewar. A dry ice/acetone bath was used for the measurements taken at 196 K, and liquid nitrogen was used for data recorded at 77 K.

Lifetime Measurement. Samples for transient luminescent decay measurements were prepared in distilled 2-MeTHF solution. The samples were deaerated by bubbling with N_2, freeze−pump−thawed (3×) and flame-sealed under vacuum. Measurements in the range of 77−300 K were performed using an Oxford OptistatDN-V cryostat instrument equipped with an intelligent temperature controller. For the temperature range of 300−378 K, the optical cell was placed in an insulated sample holder that was connected to a thermostat-controlled bath filled with a mixture of deionized water/ethylene glycol (1:1). All phosphorescent lifetimes were measured time-correlated single-photon counting using an IBH Fluorocube instrument equipped with a 405 nm (for **1**−**6**, **9**, and **10**) or a 331 nm (for **7** and **8**) LED excitation source. Fits to the temperature-dependent data were performed using the Origin (v6.1) software package.

Theoretical Calculations. All calculations were performed using the hybrid density functional theory (DFT) functional B3LYP as implemented by the Jaguar 7.0 program packages.[58] This DFT functional utilizes the Becke three-parameter functional[59] (B3) combined with the correlation functional of Lee, Yang, and Parr[60] (LYP) and is known to produce good descriptions of reaction profiles for transition metal containing compounds.[61,62] The metals were described by the Wadt and Hay[63−65] core−valence (relativistic) effective core potential (treating the valence electrons explicitly) using the LACVP basis set with the valence double-ζ contraction of the basis functions, LACVP**. All electrons were used for all other elements using a modified variant of Pople's[66,67] 6-31G** basis set, where the six d functions have been reduced to five.

(43) Kober, E. M.; Marshall, J. L.; Dressick, W. J.; Sullivan, B. P.; Caspar, J. V.; Meyer, T. J. *Inorg. Chem.* **1985**, *24*, 2755–2763.
(44) Caspar, J. V.; Kober, E. M.; Sullivan, B. P.; Meyer, T. J. *J. Am. Chem. Soc.* **1982**, *104*, 630–632.
(45) Kober, E. M.; Caspar, J. V.; Lumpkin, R. S.; Meyer, T. J. *J. Phys. Chem.* **1986**, *90*, 3722–3734.
(46) Barigelletti, F.; Sandrini, D.; Maestri, M.; Balzani, V.; von Zelewsky, A.; Chassot, L.; Jolliet, P.; Maeder, U. *Inorg. Chem.* **1988**, *27*, 3644–3647.
(47) Marchetti, A. P.; Deaton, J. C.; Young, R. H. *J. Phys. Chem. A* **2006**, *110*, 9828–9838.
(48) Rausch, A. F.; Thompson, M. E.; Yersin, H. *Inorg. Chem.* **2009**, *48*, 1928–1937.
(49) Finkenzeller, W. J.; Thompson, M. E.; Yersin, H. *Chem. Phys. Lett.* **2007**, *444*, 273–279.
(50) Finkenzeller, W. J.; Stossel, P.; Yersin, H. *Chem. Phys. Lett.* **2004**, *397*, 289–295.
(51) Finkenzeller, W. J.; Yersin, H. *Chem. Phys. Lett.* **2003**, *377*, 299–305.
(52) Harding, R. E.; Lo, S. C.; Burn, P. L.; Samuel, I. D. W. *Org. Electron.* **2008**, *9*, 377–384.
(53) Lo, S. C.; Shipley, C. P.; Bera, R. N.; Harding, R. E.; Cowley, A. R.; Burn, P. L.; Samuel, I. D. W. *Chem. Mater.* **2006**, *18*, 5119–5129.
(54) Yang, L.; Okuda, F.; Kobayashi, K.; Nozaki, K.; Tanabe, Y.; Ishii, Y.; Haga, M. A. *Inorg. Chem.* **2008**, *47*, 7154–7165.
(55) Dedeian, K.; Shi, J. M.; Shepherd, N.; Forsythe, E.; Morton, D. C. *Inorg. Chem.* **2005**, *44*, 4445–4447.
(56) Kawamura, Y.; Sasabe, H.; Adachi, C. *Jpn. J. Appl. Phys., Part 1* **2004**, *43*, 7729–7730.
(57) Demas, J. N.; Crosby, G. A. *J. Phys. Chem.* **1971**, *75*, 991–1024.
(58) Jaguar 7.0; Schrodinger, Inc.: Portland, OR, 2007.
(59) Becke, A. D. *J. Chem. Phys.* **1993**, *98*, 5648–5652.
(60) Lee, C. T.; Yang, W. T.; Parr, R. G. *Phys. Rev. B* **1988**, *37*, 785–789.
(61) Niu, S. Q.; Hall, M. B. *Chem. Rev.* **2000**, *100*, 353–405.
(62) Baker, J.; Muir, M.; Andzelm, J.; Scheiner, A. In *Chemical Applications of Density-Functional Theory*; Laird, B. B., Ross, R. B., Ziegler, T., Eds.; American Chemical Society: Washington, DC, 1996; Vol. 629, pp 342−367.
(63) Hay, P. J.; Wadt, W. R. *J. Chem. Phys.* **1985**, *82*, 299–310.
(64) Melius, C. F.; Olafson, B. D.; Goddard, W. A. *Chem. Phys. Lett.* **1974**, *28*, 457–462.
(65) Goddard, W. A. *Phys. Rev.* **1968**, *174*, 659–662.
(66) Francl, M. M.; Pietro, W. J.; Hehre, W. J.; Binkley, J. S.; Gordon, M. S.; Defrees, D. J.; Pople, J. A. *J. Chem. Phys.* **1982**, *77*, 3654–3665.
(67) Hariharan, P. C.; Pople, J. A. *Chem. Phys. Lett.* **1972**, *16*, 217–219.

Table 1. Photophysical Properties of **1**−**10** in 2-MeTHF

		77 K			298 K					
no.	complex	E_{0-0} (nm)	E_{0-0} (cm^{-1})	τ (μs)	λ_{max} (nm)	τ (air) (μs)[a]	τ (N_2) (μs)	Φ (±0.05)	k_r (s^{-1})	k_{nr} (s^{-1})
1	$Ir(ppy)_3$	491	20 370	4.0	508	0.036	1.6	0.97	6.1×10^5	1.9×10^4
2	$Ir(F_2ppy)_3$	454	22 030	2.6	466	0.037	1.7	0.98	5.8×10^5	1.2×10^4
3	$Ir(ppz)_2(ppy)$	479	20 880	4.2	500	0.038	1.7	0.95	5.6×10^5	2.9×10^4
4	$Ir(F_2ppz)_2(ppy)$	465	21 510	4.2	475	0.040	2.6	0.93	3.6×10^5	2.7×10^4
5	$Ir(ppz)_2(F_2ppy)$	463	21 600	3.4	500	0.032	1.2	0.55	4.6×10^5	3.8×10^5
6	$Ir(F_2ppz)_2(F_2ppy)$	445	22 470	3.1	457	0.044	1.3	0.60	4.6×10^5	3.1×10^5
7	$Ir(ppz)_3$	412	24 270	14			0.002	<0.01		$>10^8$
8	$Ir(F_2ppz)_3$	388	25 770	25			0.007	<0.01		$>10^8$
9	$Ir(flz)_3$	478	20 920	50	480	0.036	48	0.81	1.7×10^4	4.0×10^3
10	$Ir(pmb)_3$	378	26 455	3.1	382	0.020	1.1	0.37	3.4×10^5	5.7×10^5

[a] In toluene.

All energies here are reported as $\Delta H(0\ K) = \Delta E$ + zero-point energy correction. All geometries were optimized and evaluated for the correct number of imaginary frequencies through vibrational frequency calculations using the analytic Hessian. Zero imaginary frequencies correspond to a local minimum, whereas one imaginary frequency corresponds to a transition structure.

Results and Discussion

Luminescence data for the iridium(III) complexes **1**−**10** recorded at room temperature and 77 K in 2-MeTHF is presented in Table 1. The complexes can be divided into three different groups based on their photoluminescent quantum efficiency (Φ) at room temperature. The first four complexes (**1**−**4**) have high Φ values (0.93−0.98), a second set (**5**, **6**, **9**, and **10**) has Φ ranging between 0.30 and 0.80, and a third (**7**, **8**) has a very low Φ (<0.01). The luminescent lifetimes (τ) for **1**−**6**, **9**, and **10** fall between 1.6 and 50 μs, whereas the values for **7** and **8** are much shorter (<10 ns). Emission from all of the complexes is highly efficient at 77 K, and the luminescent lifetimes fall in the microsecond regime. The phosphorescence displayed by these iridium complexes originates from a ligand-centered triplet state (T_1) that is strongly perturbed by admixture with a state having MLCT character (^{3}MLCT-LC).[32] There is virtually no fluorescence as the rate of intersystem crossing for cyclometalated Ir complexes has been shown to be rapid (<100 fs) and, thus, near quantitative for triplet formation.[68,69]

The decay of the T_1 state to the ground state for these cyclometalated Ir complexes follows one of three paths, a temperature-dependent radiative process, $k_r(T)$, or one of two nonradiative (NR) processes, as illustrated in Scheme 1. The temperature dependence of k_r comes about from thermal population of the individual triplet substates (T_I, T_{II}, and T_{III}) of T_1, each of which has a unique radiative rate.[70] Rapid thermalization between the triplet sublevels leads to emission with characteristics of a single radiative state. The nonradiative decay has a temperature-independent process, k_{nr}, that is typically associated with vibrational deactivation.[71] The temperature-dependent process, $k_{nr}(T)$, is limited by an activation barrier of E_a separating the T_1 and NR state(s).[35,72,73] Similar

Scheme 1

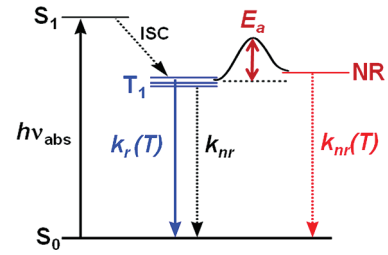

schemes have been proposed for the radiative and nonradiative decay of triplet states in Ru and Os diimmine complexes.[42,74,75]

The quantum efficiency for emission using Scheme 1 can be expressed as a function of radiative and nonradiative rates using eq 1.[35]

$$\Phi = \frac{k_r(T)}{k_r(T) + k_{nr} + k_{nr}(T)} \quad (1)$$

This equation is based on unimolecular decay, assuming contributions from second-order nonradiative decay pathways, e.g., self-quenching or quenching by impurities such as oxygen, are absent. Self-quenching can be minimized in fluid solution by performing measurements at dilute concentrations ($\leq 10^{-5}$ M). Quenching by oxygen is more problematic since these Ir compounds are quenched at near diffusion-controlled rates ($k_q = 10^9-10^{10}\ M^{-1}\ s^{-1}$),[76] as shown by the short lifetimes observed in aerated solution ($\tau = 0.020-0.044$ μs, Table 1). The rapid quenching is a consequence of deactivation by both energy and electron-transfer processes.[76,77] Electron transfer is particularly effective for these complexes since their high triplet state energies and ease of oxidation make them potent reducing agents while in the excited state. Therefore, solutions need to be vigorously deoxygenated and rigorously sealed in order to obtain reproducible values for the quantum yield. For example, we observed large decreases (>25%) within an hour during successive measurements of Φ caused by the intrusion of air when using optical cells equipped with rubber septa or poorly fitted Teflon stopcocks.

(68) Hedley, G. J.; Ruseckas, A.; Samuel, I. D. W. *Chem. Phys. Lett.* **2008**, *450*, 292–296.
(69) Tang, K. C.; Liu, K. L.; Chen, I. C. *Chem. Phys. Lett.* **2004**, *386*, 437–441.
(70) Yersin, H.; Donges, D. *Top. Curr. Chem.* **2001**, *214*, 81–186.
(71) Caspar, J. V.; Meyer, T. J. *J. Phys. Chem.* **1983**, *87*, 952–957.
(72) Caspar, J. V.; Meyer, T. J. *Inorg. Chem.* **1983**, *22*, 2444–2453.
(73) Forster, L. S. *Coord. Chem. Rev.* **2002**, *227*, 59–92.
(74) Henderson, L. J.; Fronczek, F. R.; Cherry, W. R. *J. Am. Chem. Soc.* **1984**, *106*, 5876–5879.
(75) Sauvage, J. P.; Collin, J. P.; Chambron, J. C.; Guillerez, S.; Coudret, C.; Balzani, V.; Barigelletti, F.; De Cola, L.; Flamigni, L. *Chem. Rev.* **1994**, *94*, 993–1019.
(76) Djurovich, P. I.; Murphy, D.; Thompson, M. E.; Hernandez, B.; Gao, R.; Hunt, P. L.; Selke, M. *Dalton Trans.* **2007**, 3763–3770.
(77) Schaffner-Hamann, C.; von Zelewsky, A.; Barbieri, A.; Barigelletti, F.; Muller, G.; Riehl, J. P.; Neels, A. *J. Am. Chem. Soc.* **2004**, *126*, 9339–9348.

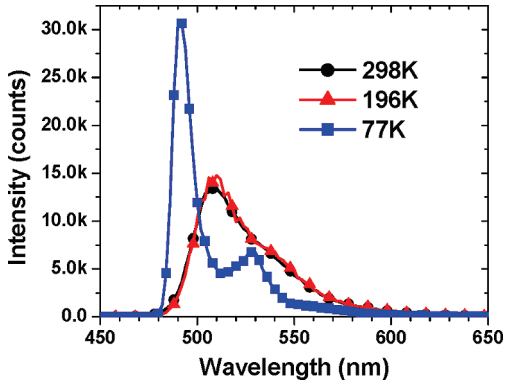

Figure 2. Emission intensity measurements of $Ir(ppy)_3$ (**1**) in 2-MeTHF at different temperatures.

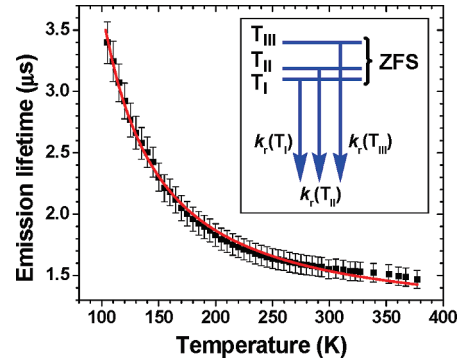

Figure 3. Temperature-dependent luminescent decay of **1**. The line is the fit to the data using a two-level Boltzmann analysis. Inset: schematic diagram illustrating the decay process from the triplet sublevels.

Given the prominence of *fac*-$Ir(ppy)_3$ (**1**) as the first reported tris-cyclometalated iridium complex,[78] and its frequent use as a primary luminescent quantum yield standard, it is important to examine the properties of this species in detail. The initial account of **1** reported its Φ as equal to 0.4 ± 0.1,[78] and this value continues to be used when the complex is employed as an emission standard. Recent measurements, either in solution or dispersed in a solid matrix, have found much higher values for Φ, ranging from 0.8 to 1.0.[1,79−81] We also obtained a quantum efficiency of near unity (0.97) for **1** in toluene and 2-MeTHF solutions. These high values suggest that the nonradiative channels are not available (i.e., $k_{nr} \ll k_r$) and will likely not become active as the temperature is lowered. To confirm this hypothesis, the emission intensity of **1** was measured in 2-MeTHF at three different temperatures: 298, 195, and 77 K (Figure 2). Although the emission line shape undergoes a blue shift and the vibronic structure is better resolved upon freezing of the solvent, there is no change in integrated emission intensity as the temperature is lowered; the peak areas are within 1.5% ($6.4-6.5 \times 10^5$ counts). This result agrees with other studies that also show luminescence of **1** doped in a solid matrix displays no variation in intensity between room temperature and 4 K.[81,82]

Although the quantum yield for **1** remains constant below 300 K, the luminescent lifetime, and thus the radiative rate, does vary with temperature. The lifetimes of **1** at 298, 195, and 77 K are 1.6, 1.8, and 4.0 μs, respectively. It is worth noting that the 2.5 times increase in lifetime upon cooling to 77 K was used to provide support for the initial determination of $\Phi = 0.4$.[78] Such an interpretation requires that the radiative rate be temperature-independent, an assumption commonly invoked when describing k_r values for phosphorescence. This assumption, however, is only valid for species with small values of zfs between the triplet substates. For compounds with a zfs less than $3k_BT$, thermal equilibration of the individual triplet sublevels is rapid and phosphorescence can be treated as originating from a single state, having an average $k_r = 1/3[k_r(T_I) + k_r(T_{II}) + k_r(T_{III})]$.[83] Since most organic compounds have small values for zfs (<1 cm^{-1}), thermal equilibration of the triplet substates occurs at temperatures well below 77 K. The values of zfs for transition metal complexes that have significant contributions of MLCT character in their excited state are markedly larger than those of organic materials, reaching values >200 cm^{-1}.[23] Thus, thermal equilibration of the triplet sublevels for metal complexes, such as cyclometalated Ir(III) complexes, can require temperatures well above 77 K. In order to estimate the zfs for **1**, a two-level Boltzmann analysis was performed on the luminescent decay using data taken in the temperature range of 77−378 K. The analysis gives a value for k_1 of 1.8×10^{-6} s^{-1} and activation energy (E_a) of 122 cm^{-1} (Figure 3). The k_1 value represents the high-temperature limit to the radiative rate, whereas E_a corresponds to the zfs between the T_I and T_{III} triplet substates, inset to Figure 3. The smaller splitting between sublevels T_I and T_{II} could not be resolved in this temperature range. The k_1 and E_a values are in good agreement with results obtained by Yersin from observations of *fac*-$Ir(ppy)_3$ taken in THF at lower temperatures, where $k_r(T_{III}) = 1.3 \times 10^{-6}$ s^{-1} and the zfs was found to be site-dependent and range between 90 and 150 cm^{-1}.[84,85] The decrease in lifetime observed upon warming **1** from 77 to 298 K is thus due to an increase in the radiative rate caused by thermal population of the higher triplet sublevels, particularly the T_{III} substate responsible for fast radiative decay.

The high quantum efficiency at room temperature of **1** indicates that the overall nonradiative decay rate ($k_{nr} + k_{nr}(T)$) for this complex is at least 2 orders of magnitude smaller than the radiative decay rate ($k_r = 7.5 \times 10^5$ s^{-1}, Table 1). The near unit value for Φ sets an upper limit for $k_{nr} + k_{nr}(T)$, dictated by the precision of the quantum yield measurement, to be less than 3.0×10^4 s^{-1}. Such a low rate implies that neither temperature-independent nor temperature-dependent nonradiative decay is effective at deactivating the excited state for **1** at temperatures of 300 K and below.

Temperature-independent nonradiative decay can occur through two different pathways: direct surface crossing from T_1 and S_0

(78) King, K. A.; Spellane, P. J.; Watts, R. J. *J. Am. Chem. Soc.* **1985**, *107*, 1431–1432.
(79) Kawamura, Y.; Goushi, K.; Brooks, J.; Brown, J. J.; Sasabe, H.; Adachi, C. *Appl. Phys. Lett.* **2005**, *86*, 071104.
(80) Holzer, W.; Penzkofer, A.; Tsuboi, T. *Chem. Phys.* **2005**, *308*, 93–102.
(81) Tanaka, I.; Tabata, Y.; Tokito, S. *Jpn. J. Appl. Phys., Part 2* **2004**, *43*, L1601–L1603.
(82) Goushi, K.; Kawamura, Y.; Sasabe, H.; Adachi, C. *Jpn. J. Appl. Phys., Part 2* **2004**, *43*, L937–L939.
(83) Tinti, D. S.; El-Sayed, M. A. *J. Chem. Phys.* **1971**, *54*, 2529–2549.
(84) The value for the zfs of *fac*-$Ir(ppy)_3$ is reported to be 83 cm^{-1} in ref 50. Subsequent re-examination of the complex in THF has found the zfs to vary between 90 and 150 cm^{-1}, depending on the site occupied in the solvent lattice. Hofbeck, T.; Yersin, H. *3rd International Symposium on Molecular Materials−MOLMAT, Book of Abstracts*; Toulouse, France, July 8−11, 2008; p 157.
(85) Goushi, K.; Brooks, J.; Brown, J. J.; Sasabe, H.; Adachi, C. *J. Photopolym. Sci. Technol.* **2006**, *19*, 181–186.

Table 2. Kinetic Parameters for the Excited-State Decay of **1**−**10** in 2-MeTHF

no.	complex	k_1 (s^{-1})	E_{a1} (cm^{-1})	k_2 (s^{-1})	E_{a2} (cm^{-1})	$E_{0-0} + E_{a2}$ (cm^{-1})	Φ
1	$Ir(ppy)_3$	1.8×10^6	120				0.97
2	$Ir(F_2ppy)_3$	1.5×10^6	50	6.2×10^{11}	4200	26 230	0.98
3	$Ir(ppz)_2(ppy)$	1.6×10^6	120	4.0×10^{14}	4800	25 680	0.95
4	$Ir(F_2ppz)_2(ppy)$	8.5×10^5	50	3.4×10^{13}	4600	26 110	0.93
5	$Ir(ppz)_2(F_2ppy)$	1.1×10^6	90	5.0×10^{12}	3300	24 900	0.55
6	$Ir(F_2ppz)_2(F_2ppy)$	1.2×10^6	60	6.1×10^{12}	3500	25 970	0.60
7	$Ir(ppz)_3$	2.5×10^5	60	1.2×10^{12}	1800	26 070	<0.01
8	$Ir(F_2ppz)_3$	2.1×10^5	90	2.6×10^{11}	1600	27 370	<0.01
9	$Ir(flz)_3$	4×10^4	<10				0.81
10	$Ir(pmb)_3$	8.3×10^5	40	3.7×10^9	1700	28 155	0.37

and/or vibrational coupling to the ground state. The former process can be excluded from consideration due to the vibronic structure of the emission spectra, which indicates no major structural distortion occurs in the ligand-localized excited state relative to the ground state. Therefore, the only available temperature-independent mechanism is vibrational coupling to the ground state, which is governed by the energy gap law (EGL).[86,87] Compounds that follow the EGL show a linear decrease in $\ln(k_{nr})$ with increasing emission energy. Numerous studies have shown that the nonradiative rates of luminescent d^6 metal complexes follow EGL behavior.[44,45,71] Typically, high-frequency metal−ligand or C−C skeletal stretching vibrations provide the most effective deactivation mode to couple the ground and excited states. In particular, extensive work by Meyer and co-workers has generated enough data to allow us to predict the k_{nr} values for blue phosphors.[45,71] A linear extrapolation to high energy (>20 000 cm^{-1}, 2.48 eV) of the EGL using slope (−7.5 $\ln(k_{nr})$/eV) and intercept (29.2) data for red emissive Os(II) bipyridyl complexes[88] leads to values of k_{nr} less than 4.0×10^4 s^{-1}. The phenomenon is exemplified by *fac*-$Ir(flz)_3$ (**9**), where the $k_{nr} = 4.0 \times 10^3$ s^{-1}. Given the high k_r values (>10^5 s^{-1}) found for most of the other cyclometalated Ir complexes, simple vibrational deactivation processes should have a minor impact on the value of Φ. It follows then, that the principal mechanism that promotes nonradiative decay, lowering the quantum efficiency of complexes **3**−**8** and **10**, is thermal population of the NR state(s), Scheme 1.

In order to gain a better understanding of the thermally activated nonradiative decay processes in these materials, luminescent lifetimes for **2**−**10** were measured between 77 and 398 K. Kinetic parameters for the luminescent decay in 2-MeTHF solution were obtained by fitting data plotted as $1/\tau$ versus T using a Boltzmann model incorporating two temperature-dependent terms, eq 2, where τ = experimental luminescent lifetime at temperature T, k_0 = decay rate at for the lowest energy triplet substate, k_1, k_2 = decay rate constants, E_{a1}, E_{a2} = activation energies, and k_B = Boltzmann constant. Inclusion of a third term to the equation did not improve the fit. The results of the fitting of experimental data to eq 2 are summarized in Table 2. The fitting procedure required the value for k_0 to be fixed in order to obtain reasonable values for the kinetic parameters. An estimate for $k_0 = 10^4$ s^{-1} was used for this purpose and is based on values of $\tau = 45-300$ μs obtained for other Ir cyclometalated complexes at temperatures below 15 K.[47−51,85,89] Varying k_0 by ±5000 s^{-1} did not significantly alter the results given in Table 2.

$$\tau = 1/k_{observed} = \frac{1 + \exp(-E_{a1}/k_BT) + \exp(-E_{a2}/k_BT)}{k_0 + k_1 \exp(-E_{a1}/k_BT) + k_2\exp(-E_{a2}/k_BT)} \quad (2)$$

Plots of temperature versus the decay rate display two distinct regimes, one at low temperature that corresponds to thermal redistribution between the triplet sublevels (dependent on the zfs) and the other at higher temperature that involves population of a nonradiative state. Figure 4 shows the data and fits for complexes **3** and **5**. The decay rate constants (k_1) obtained from the low-temperature regime are between 10^5 and 10^6 s^{-1} for **1**−**8** and **10**, while the values of E_{a1} fall within the range of 40−120 cm^{-1}. The values for **9** are lower ($k_1 = 10^4$ s^{-1}, $E_{a1} <$ 10 cm^{-1}). The data for E_{a1} should reflect the zfs between the T_I and T_{III} triplet substates and are comparable to values reported for other cyclometalated Ir(III) complexes.[47,49,50,89] Large values of zfs have been correlated with an increasing degree of MLCT character in the excited state.[90] The low E_{a1} value for **9**, coupled with its low radiative rate, is consistent with a relatively small MLCT contribution to the ^{3}MLCT-LC state for this complex.

The activation energy to populate the NR state (E_{a2}, labeled E_a in Scheme 1) was determined from the temperature-dependent decay rate. The values of E_{a2} for **2**−**8** and **10** vary between 1600 and 4800 cm^{-1} (Table 2). The decay rate constant of the NR state (k_2) for **2**−**8** are all $10^{11}-10^{14}$ s^{-1}, whereas the value for **10** is slower ($\sim 10^9$ s^{-1}). No thermal activation to an NR state is observed for either **1** or **9**. For **1**, the only thermally activated phenomenon observed within the limit of our measurement (77−398 K) is the variation in the radiative rate due to the equilibrating triplet sublevels. Likewise for **9**, an efficient blue-green phosphor (Φ = 0.81), the only temperature-dependent phenomena observed between 77 and 298 K appears to originate from thermal population of the triplet substates. However, data from **9** was less reproducible than that from the other cyclometalated species as this complex has a relatively long lifetime ($\tau_{298K} = 48$ μs, Table 1) that makes it extremely susceptible to quenching by oxygen ($k_q = 1.5 \times 10^{10}$ M^{-1} s^{-1}; Stern−Volmer quenching constant, $k_q\tau_{298K} = 7.2 \times 10^5$ M^{-1}) and other impurities. The high sensitivity to quenching from water or other spurious impurities released on flame-sealing samples of **9** made it difficult to precisely monitor temperature-dependent variations in the luminescent decay using our experiment setup.

The luminescent quantum efficiency for complexes **2**−**8** and **10** is determined principally by the activation energy to the NR state. Complexes **2**−**4** have high Φ (>0.93) and values of E_{a2} (>4000 cm^{-1}) that are large enough to make the NR state thermally accessible only at temperatures greater than 300 K,

(86) Freed, K. F.; Jortner, J. *J. Chem. Phys.* **1970**, *52*, 6272–6291.
(87) Englman, R.; Jortner, J. *Mol. Phys.* **1970**, *18*, 145–164.
(88) Allen, G. H.; White, R. P.; Rillema, D. P.; Meyer, T. J. *J. Am. Chem. Soc.* **1984**, *106*, 2613–2620.
(89) Rausch, A. F.; Homeier, H. H. H.; Djurovich, P. I.; Thompson, M. E.; Yersin, H. *Proc. SPIE—Int. Soc. Opt. Eng.* **2007**, *6655*, 66550F.
(90) Yersin, H.; Humbs, W. *Inorg. Chem.* **1999**, *38*, 5820–5831.

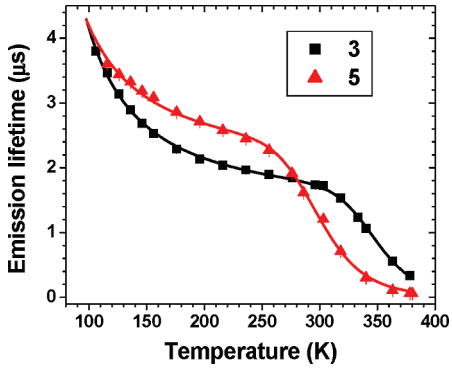

Figure 4. Temperature dependence of luminescence decay rate for **3** and **5**, illustrating zfs dominated decay from 100 to 250 °C and $k_{nr}(T)$-dependent decay >250 °C. Lines are fits to the data using eq 2.

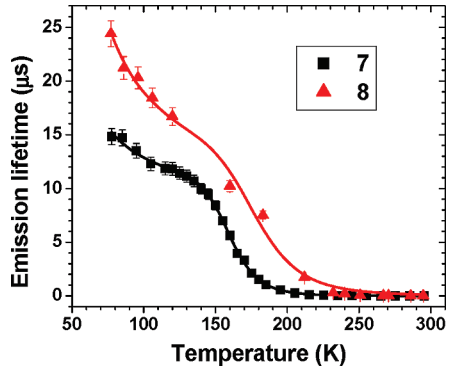

Figure 5. Temperature-dependent luminescent decay of **7** and **8**, illustrating zfs dominated decay from 77 to 100 °C and $k_{nr}(T)$-dependent decay >150 °C. Lines are fits to data using eq 2.

whereupon there is a marked decrease in the luminescent lifetime (e.g., see **3** in Figure 4). Complexes **5** and **6** with moderate quantum efficiency ($\Phi = 0.55$ and 0.60, respectively) have intermediate values for E_{a2} (~3400 cm^{-1}). The temperature-dependent lifetime data for both of these complexes show that the NR state is accessible at room temperature (e.g., **5** in Figure 4).

Complexes **7** and **8** are effectively nonemissive at room temperature ($\Phi < 0.001$), with small E_{a2} values (1800 cm^{-1} for **7**, 1600 cm^{-1} for **8**). Thermally activated decay from the NR state is highly effective even below room temperature (Figure 5). Both **7** and **8** are strongly emissive at 77 K, and the luminescent lifetimes show marked increase upon cooling from 298 to 77 K: from 0.002 to 14 μs for **7** and 0.007 to 25 μs for **8**. Finally, for *fac*-Ir(pmb)$_3$ (**10**), although the activation energy is small ($E_{a2} = 1700$ cm^{-1}) the quantum efficiency is relatively high ($\Phi = 0.37$). Despite having a similar value of E_{a2} to that of nonemissive **7**, the luminescent lifetime for **10** displays only a moderate dependence on temperature ($\tau_{298K} = 1.1$ μs, $\tau_{77K} = 3.1$ μs). The reason for this insensitivity is the markedly smaller pre-exponential term for **10** ($k_2 = 3.7 \times 10^9$ s^{-1}), which also allows for moderately efficient emission to occur at room temperature.

The variation in the thermally activated kinetic parameters for luminescent decay provides some clues as to the nature of the NR state. The height of the barrier to reach the NR state from the ground state for **7** ($E_{0-0} + E_{a2} = 26\,070$ cm^{-1}, 75 kcal/mol) is close to the strength of an Ir−C_{phenyl} bond (80 kcal/mol).[91] The energy barrier to the NR state for **10** ($E_{0-0} + E_{a2} = 28\,155$ cm^{-1}, 80 kcal/mol) is also comparable to the bond strength calculated for a Ir−C_{phenyl} and Au−$C_{carbene}$ linkages (65−88 kcal/mol).[92,93] Given these energies, a process involving Ir−ligand bond rupture is a likely path to the NR state. Additional support for ligand dissociation comes from studies on luminescent Ru diimine complexes, where studies suggested that photosubstitution reactions in these species coincide with thermal activation to the nonradiative states.[94] A signature for a dissociative state in the Ru complexes is the magnitude of the pre-exponential term for thermal deactivation (k_2).[95] Large values of k_2 ($10^{11}-10^{14}$ s^{-1}), similar to those is found for **2**−**8**, are associated with high-frequency vibrations and consistent with bond rupture being involved in the luminescent deactivation process.

A recent publication discussing DFT calculation for **1** and **7** provides additional support for the participation of a ligand dissociation process in the excited state.[96] According to these calculations, the most favorable (lowest energy) triplet state of **7** has a five-coordinate structure, formed upon breaking an Ir−N bond of one phenylpyrazolyl ligand. On the basis of these results, we carried out DFT calculations, using a B3LYP/LACVP** model, for the triplet states of six- and five-coordinated variants of **1**−**10**. Selected metrical and thermodynamic data calculated for the complexes are presented in Supporting Information Tables S1 and S2, respectively. A distorted octahedral geometry around the metal center, similar to that determined for the singlet state, was found for all of the six-coordinate species. One of the chelates has metal−ligand bonds that are ca. 0.03−0.05 Å shorter than those found in the other two ligands. The spin density surface is primarily localized on this distorted ligand, along with a small contribution from the metal center, and is compatible with a ^{3}MLCT-LC description of the excited state. The structures for the five-coordinate species were obtained from an unrestricted geometry optimization calculation, performed from a starting point generated by breaking an Ir−N (or Ir−$C_{carbene}$ for **10**) bond and rotating the unligated heterocyclic to a dihedral angle of 90°, relative to the phenyl group. All the five-coordinate intermediates were verified to be local minima by vibrational analysis. Structures with lowest energy were found for the rotomer with the unbound nitrogen oriented toward a hydrogen atom on the heterocycle of an adjacent chelate (Figure 6).

The geometry around the metal center for the five-coordinate species closely matches that reported earlier for **1** and **7**[96] and is best described as a distorted trigonal bipyramid (TBP) with an equatorial plane containing two phenyl groups and a heterocycle of a chelating ligand, see Scheme 2. Previous work by Eisenstein has shown that the triplet state of d^6 ML_5 complexes is Jahn−Teller active and that the presence of three strong σ-donating ligands in the equatorial plane favors the TBP geometry over a square pyramidal structure.[97] For the hetero-

(91) Nolan, S. P.; Hoff, C. D.; Stoutland, P. O.; Newman, L. J.; Buchanan, J. M.; Bergman, R. G.; Yang, G. K.; Peters, K. S. *J. Am. Chem. Soc.* **1987**, *109*, 3143–3145.
(92) Scott, N. M.; Dorta, R.; Stevens, E. D.; Correa, A.; Cavallo, L.; Nolan, S. P. *J. Am. Chem. Soc.* **2005**, *127*, 3516–3526.
(93) Hu, X. L.; Castro-Rodriguez, I.; Olsen, K.; Meyer, K. *Organometallics* **2004**, *23*, 755–764.
(94) Durham, B.; Caspar, J. V.; Nagle, J. K.; Meyer, T. J. *J. Am. Chem. Soc.* **1982**, *104*, 4803–4810.
(95) Barigelletti, F.; Juris, A.; Balzani, V.; Belser, P.; Vonzelewsky, A. *J. Phys. Chem.* **1987**, *91*, 1095–1098.
(96) Treboux, G.; Mizukami, J.; Yabe, M.; Nakamura, S. *Chem. Lett.* **2007**, *36*, 1344–1345.
(97) Riehl, J. F.; Jean, Y.; Eisenstein, O.; Pelissier, M. *Organometallics* **1992**, *11*, 729–737.

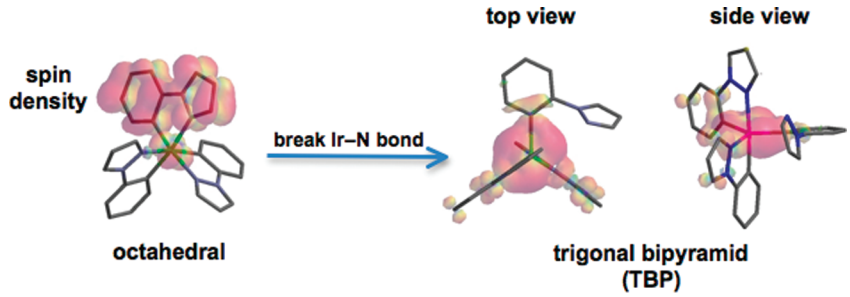

Figure 6. Structures and spin density surfaces calculated for the triplet states of six- and five-coordinated forms of **7**.

Scheme 2

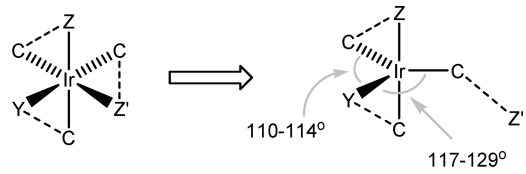

C = phenyl, Y = pyridyl, Z, Z' = pyrazolyl

Table 3. Calculated Energy Parameters for the Triplet State of **1**−**10**

no.	complex	ΔH (cm^{-1})	$E_{a2} - \Delta H$ (cm^{-1})	$E_{0-0} + \Delta H$ (cm^{-1})
1	Ir(ppy)$_3$	2117		22 487
2	Ir(F$_2$ppy)$_3$	1754	2416	23 784
3	Ir(ppz)$_2$(ppy)	1042	3788	21 922
4	Ir(F$_2$ppz)$_2$(ppy)	1655	2945	23 165
5	Ir(ppz)$_2$(F$_2$ppy)	130	3170	21 730
6	Ir(F$_2$ppz)$_2$(F$_2$ppy)	766	2744	23 236
7	Ir(ppz)$_3$	−1676	3496	22 594
8	Ir(F$_2$ppz)$_3$	−1719	3279	24 051
9	Ir(flz)$_3$[a]	1137		22 057
10	Ir(pmb)$_3$	1557	143	28 012

[a] 9,9′-Dihydro analogue of flz ligand.

leptic compounds **3**−**6**, the lowest energy was found for a structure formed by breaking the Ir−N$_{pyrazole}$ bond that is trans to the phenyl of an adjacent ppz ligand (Ir−Z′, Scheme 2), an arrangement that places the chelated pyridyl ligand at an equatorial site. The N−Ir−C equatorial angle between the chelated ligands falls in a narrow range (110−114°) and is smaller than the C−Ir−C and N−Ir−C equatorial angles to the monodentate ligand (117−129°). The dihedral angle between the phenyl and heterocycle for the monodentate ligand is >50° for **1**−**10**. The spin density is localized within the equatorial plane for the TBP geometry (Figure 6), and the density at the metal center (0.81−1.11) is significantly larger than for the octahedral form (0.12−0.48), a picture consistent with a description of the TBP intermediate as a ^{3}MC state.

A key parameter to characterize the ^{3}MC state obtained from the calculations is ΔH, the difference in energy between the zero-point energies (zpe) calculated for the triplet states of the octahedral and TBP geometries of a respective complex (Table 3). The value of ΔH defines the relative thermodynamic stability of luminescent triplet state with respect to the product of bond rupture and originates from the differing orbital nature of the two states. The energy of the ^{3}MLCT-LC state in the octahedral form is primarily dictated by the triplet energy of cyclometalated ligand, which can vary considerably depending on the identity of the cyclometalate. On the other hand, the energy of the ^{3}MC state in the TBP intermediate is mostly metal-centered and, thus, determined mainly by the ligand field strength of the coordinating ligands, particularly the ones in the equatorial plane (two phenyls and one imine). For example, the energy of ^{3}MLCT-LC state (E_{0-0}) increases by 3900 cm^{-1} upon going from **1** (ppy ligand) to **7** (ppz ligand), whereas the calculated energy of the ^{3}MC state ($E_{0-0} + \Delta H$) for the TBP form increases only slightly, by ∼100 cm^{-1}. A similar difference in triplet energy occurs between the ^{3}MLCT-LC state of **2** and **8** (3740 cm^{-1}) and the ^{3}MC state (267 cm^{-1}). For compounds **1**−**9**, a plot of ΔH versus E_{0-0} (Figure 7) displays the trend of decreasing ΔH with increasing emission energy. The variation in ΔH with respect to emission energy indicates that, for a particular compound, the TBP intermediate is destabilized to a lesser extent by the various ligands than is the octahedral form. In other words, higher emission energies thermodynamically favor the ^{3}MC state over the ^{3}MLCT-LC state. Two different trend lines can be discerned in the plot, for complexes either with difluorophenyl groups in the equatorial plane of the TBP intermediate (**2**, **4**, **6**, and **8**, blue in Figure 8) or with phenyl groups (**1**, **3**, **5**, **7**, and **9** colored red in the plot). This segregation of data indicates that the difluorophenyl groups exert an equivalent destabilizing effect on both the ^{3}MLCT-LC and ^{3}MC states relative to the respective nonfluorinated complexes.

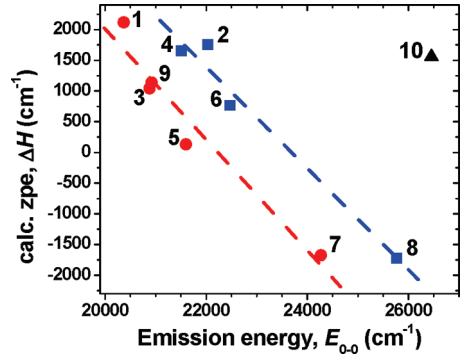

Figure 7. Plot of the emission energy (E_{0-0}) vs ΔH for **1**−**10**. Compounds with phenyl ligands in the equatorial plane of the TBP structure are shown in red, those with F$_2$phenyl are in blue. The lines are just guides for the eye.

The value of ΔH can also be correlated with the activation energy (E_{a2}). Note, for example, that compound **1**, with the largest value for ΔH (2117 cm^{-1}), has an E_{a2} that is inaccessible even at 378 K. The correspondence between E_{a2} and ΔH is shown for compounds **2**−**8** and **10** in Figure 8. The decrease in E_{a2} with decreasing ΔH is a consequence of the deviation between ^{3}MLCT-LC and ^{3}LC energies of the two different excited-state geometries of the complexes. The activation energy will decrease as the octahedral form becomes thermodynamically destabilized (less favored) relative to the TBP intermediate (smaller ΔH). The trend displayed in Figure 8 also indicates that the driving force to reach the TBP intermediate is correlated

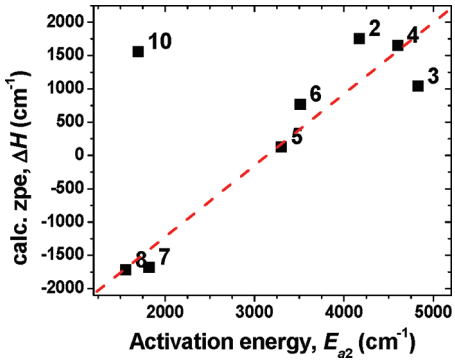

Figure 8. Plot of the activation energy (E_{a2}) vs ΔH for **2**−**8** and **10**. The line is just a guide for the eye.

with the luminescent quantum efficiency. Compounds with large ΔH (**1**−**4**) have high Φ, those with small ΔH (**5** and **6**) have moderate efficiency, and complexes with a negative ΔH (**7** and **8**) are nonemissive at room temperature.

For compound **10**, the relationships between E_{a2}, ΔH, and Φ do not follow the same trend as for the other complexes. The value of E_{a2} is similar to that of complexes with low Φ (**7** and **8**), yet the value of ΔH is comparable to that of complexes with much higher Φ, such as **2** and **3**. The discrepancy can be explained using a kinetic scheme, analogous to one first proposed by Meyer for Ru(diimine) complexes,[94] where the ^{3}MLCT-LC state is in equilibrium with the ^{3}MC state before undergoing irreversible return to the ground state (eq 3).[40]

$$^3\text{MLCT-LC}_{\text{octahedral}} \underset{k_b}{\overset{k_a}{\rightleftharpoons}} {}^3\text{MC}_{\text{TBP}} \xrightarrow{k_c} S_0 \qquad (3)$$

In the case where $k_c \gg k_b$, the formation of the ^{3}MC state will be the rate-limiting step. Upon entering the ^{3}MC channel, back-reaction will not occur as the complex will undergo rapid intersystem crossing and nonradiative return to the ground state. This interpretation of the excited-state behavior is in line with the thermally activated properties exhibited by complexes **3**−**8**, such as the large magnitude for the pre-exponential term ($k_2 > 10^{11}$ s^{-1}). However, as the energy barrier to back-reaction ($E_{a2} - \Delta H$) is lowered, the rate of k_b will increase to the point where it will become much greater than k_c and compete effectively with nonradiative decay. The data for **10** is consistent for a case where k_b has increased such that $k_b \gg k_c$. The barrier for back-reaction for this complex is so low ($E_{a2} - \Delta H = 143$ cm^{-1}, Table 3) that return to the ^{3}MLCT-LC state decreases the value of ln(k_2). From the near-zero value of $E_{a2} - \Delta H$ for **10**, one can also estimate a value of $k_c \approx 10^9$ s^{-1}. This value is 10^4 times faster than the radiative rate ($k_r = 3.4 \times 10^5$ s^{-1}, Table 1), which still makes population of the ^{3}MC state a viable nonradiative decay process.

The data for the experimental and calculated energetic parameters for the excited states of **1**−**8** and **10** is summarized in Figure 9. The $E_{0-0} + E_{a2}$ data represents the energy of the transition state, whereas the $E_{0-0} + \Delta H$ data provides an estimate for the energy of the ^{3}MC state (E_a and NR in Scheme 1, respectively). Figure 9 readily illustrates that the energy of the ^{3}MC state is confined to a narrower range of values (2300 cm^{-1}) for the ppy and ppz derivatives than is the ^{3}MLCT-LC state (5400 cm^{-1}). The tight energy distribution for the ^{3}MC state of complexes **1**−**8** implies a thermodynamic limit (~24 000 cm^{-1}, 415 nm) to the stability of the ^{3}MLCT-LC excited state, and consequently the luminescent efficiency, that can be

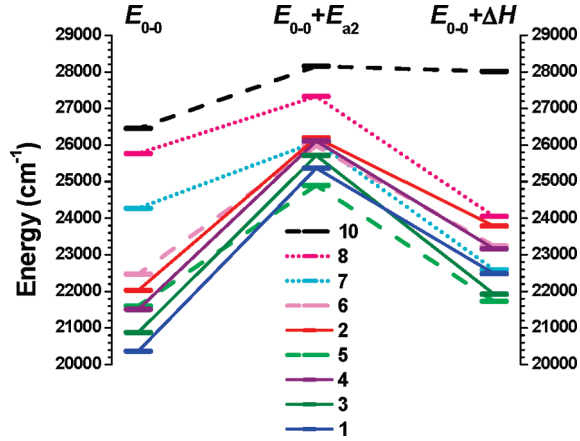

Figure 9. Summary of the temperature-dependent energetic parameters for **1**−**8** and **10**. The E_{a2} value for **1** was estimated to be 5000 cm^{-1} from data in Figure 8. The lines connecting the states distinguish the compounds as having either a high (solid, $\Phi > 0.9$), intermediate (dash, $\Phi = 0.3-0.6$), or low (dot, $\Phi < 0.01$) quantum efficiency at room temperature.

achieved for tris-cyclometalated complexes with these types of heterocyclic ligands. However, the high energy of $E_{0-0} + \Delta H$ for **10** suggests that heteroleptic complexes with carbene ligands can provide correspondingly high ^{3}MC state energies that could lead to deep-blue phosphorescent materials with efficiencies similar to values found for **1**−**4**.

Conclusion

In conclusion, analysis of the temperature dependence of luminescence from high-energy (sky-blue to near-UV) phosphorescent, tris-cyclometalated iridium complexes uncovers several important aspects regarding the triplet excited state. Once radiative rates reach values of 10^5 s^{-1}, as typically observed for these species, vibrational coupling to the ground state is not a competitive deactivation pathway for nonradiative decay. If no other unimolecular quenching process is available for these complexes, the luminescent quantum yields can approach unity, a situation that occurs for *fac*-Ir(ppy)$_3$ (**1**). One consequence of this result is the need to re-examine previous data reported for the luminescent characteristics of transition metal complexes. In the past several years the widespread use of an earlier, lower value ($\Phi = 0.4$) when using **1** as a primary quantum yield standard has led to an accumulation of errors in the literature values for the photophysical properties of a large number of related phosphorescent materials. Adoption of the higher value for the quantum yield should be employed in future work, and previous literature data that used the lower number needs to be re-evaluated with an appropriate degree of skepticism.

The temperature-dependent behavior for compounds **2**−**8** and **10** reveals decreases in luminescent efficiency caused by the presence of a thermally activated, nonradiative decay channel. Correlations between kinetic parameters and theoretical modeling suggest that deactivation occurs via a five-coordinate species formed by rupture of an Ir−N (Ir−C$_{\text{carbene}}$ in **10**) bond. DFT calculations for the five-coordinate intermediates are consistent with a description of the electronic structure as a ^{3}MC state. Inhibition of the bond rupture process in these types of high-energy phosphorescent complexes is expected to lead to materials with higher luminescent efficiencies. One approach to achieve this goal is to incorporate ligands that increase the energy of the ^{3}MC

state and thereby raise the height of the barrier needed to thermally deactivate the complex. This can be accomplished, for example, by using cyclometalated carbenes as ancillary ligands.[31] Another method is to use rigid ligands that limit the degrees of freedom needed to dissociate a metal−ligand bond. This could involve cyclometalating ligands similar 7,8-benzoquinoline[98] or the use tripodal type chelates in order to form a hemicage structure around the complex.[77] The use of a rigid matrix is an additional method that has been shown to inhibit the thermal deactivation process in luminescent transition metal complexes.[34,99] Any combination of these approaches could be employed to create high-performance blue phosphors in the future, by selecting for materials that inhibit a bond rupture pathway in their excited-state potential energy surface.

Acknowledgment. We would like to acknowledge Universal Display Corporation and Department of Energy for their financial support of this work. We also thank W. J. Finkenzeller and Professor H. Yersin (U. Regensburg) and Professor K. Dedeian (Delaware Valley College) for helpful discussions.

Supporting Information Available: Plots for the temperature dependence of emission lifetime for **2**, **4**, **6**, and **10**, tables of selected metrical parameters calculated for the triplet states of **1**−**10**, *xyz* coordinates for the calculated structures of **1**−**10**. This material is available free of charge via the Internet at http://pubs.acs.org.

JA903317W

(98) Lamansky, S.; Djurovich, P.; Murphy, D.; Abdel-Razzaq, F.; Kwong, R.; Tsyba, I.; Bortz, M.; Mui, B.; Bau, R.; Thompson, M. E. *Inorg. Chem.* **2001**, *40*, 1704–1711.

(99) Thompson, D. W.; Fleming, C. N.; Myron, B. D.; Meyer, T. J. *J. Phys. Chem. B* **2007**, *111*, 6930–6941.